Bifurcation scenarios for bubbling transition

Aleksey V. Zimin*
Department of Physics, Box 240, Physics Building, University of Maryland, College Park, Maryland 20742

Brian R. Hunt
Institute for Physical Science and Technology and Department of Mathematics, University of Maryland, College Park, Maryland 20742

Edward Ott
Institute for Research in Electronics and Applied Physics, Department of Physics and Department of Electrical and Computer Engineering, University of Maryland, College Park, Maryland 20742

(Received 11 September 2002; published 8 January 2003)

Dynamical systems with chaos on an invariant submanifold can exhibit a type of behavior called bubbling, whereby a small random or fixed perturbation to the system induces intermittent bursting. The bifurcation to bubbling occurs when a periodic orbit embedded in the chaotic attractor in the invariant manifold becomes unstable to perturbations transverse to the invariant manifold. Generically the periodic orbit can become transversely unstable through a pitchfork, transcritical, period-doubling, or Hopf bifurcation. In this paper a unified treatment of the four types of bubbling bifurcation is presented. Conditions are obtained determining whether the transition to bubbling is soft or hard; that is, whether the maximum burst amplitude varies continuously or discontinuously with variation of the parameter through its critical value. For soft bubbling transitions, the scaling of the maximum burst amplitude with the parameter is derived. For both hard and soft transitions the scaling of the average interburst time with the bifurcation parameter is deduced. Both random (noise) and fixed (mismatch) perturbations are considered. Results of numerical experiments testing our theoretical predictions are presented.

DOI: 10.1103/PhysRevE.67.016204 PACS number(s): 05.45.Xt

I. INTRODUCTION

In this paper we will be concerned with dynamical systems that contain an invariant manifold [1] embedded in their phase space and for which there exists a chaotic attractor in the invariant manifold. Such systems are common in a variety of physical situations, and they display interesting dynamical behaviors. Types of such dynamical behavior include on-off intermittency [2], riddled basins of attraction [3], and bubbling [4–8]. Examples of systems having invariant manifolds include systems with spatial symmetry [9], predator-prey models [10], magnetic dynamos [11], and synchronized chaotic oscillators [12]. The subject of this paper is the transition to bubbling. Following [4], we introduce a *normal* parameter—a parameter whose variation affects the system dynamics off the invariant manifold but leaves the dynamics within the invariant manifold unchanged. For example, in the case of synchronization of two coupled chaotic oscillators [as in Eqs. (1)], the coupling strength is the normal parameter. The bubbling transition occurs when, as a normal parameter is varied, a periodic orbit embedded within the chaotic attractor first becomes unstable to perturbations transverse to the invariant surface [13]. Before the transition, all periodic orbits in the chaotic attractor are transversely stable. Beyond the bubbling transition, if the system is perturbed in a direction transverse to the invariant manifold, orbits that come close to the transversely unstable periodic orbits are repelled and move away from the invariant manifold. If there is no other attractor off the invariant manifold, the orbit returns, and, assuming that the perturbations continue, this process repeats, producing intermittent bursts away from the invariant manifold. If, on the other hand, there is another attractor not on the invariant manifold, orbits initially repelled from the periodic orbit on the invariant manifold may go to that attractor and never return. For definiteness, the following discussion will not consider the case where there is another attractor not on the invariant manifold, although later on in the paper (Sec. VII) we indicate how our results carry over to this case.

We consider the dependence of bursting on two parameters: the normal parameter and the size of perturbations transverse to the invariant manifold. These perturbations, which we assume to be small, may be random (noise) or fixed (as in the case of coupled oscillators when there may be a slight mismatch between the two oscillators). For a given fixed value of the normal parameter beyond the bubbling transition, as the size of the perturbations goes to zero, the typical size of bursts remains finite. Thus we can define a maximum burst amplitude as a function of the normal parameter as the maximum size of bursts in the limit as the perturbation size goes to zero.

We distinguish between two types of bubbling transition: soft and hard. When a soft bubbling transition occurs, the maximum burst amplitude increases continuously from zero as the value of the system's normal parameter goes through its critical value. When a hard transition occurs, the maximum burst amplitude increases discontinuously from zero to a finite value at the bifurcation.

*Corresponding author. FAX: (301)314-9363. Email address: alekseyz@physics.umd.edu

In this paper we investigate the transition to bubbling as the normal parameter of the system goes through its critical value and find the conditions on the other parameters of the system leading to soft or hard transitions. We present results for the dependence of the maximum burst amplitude on the normal parameter for a soft transition and the dependence of the average interburst time on the normal parameter and the size of the perturbations for both hard and soft transitions. As previously mentioned, the bubbling transition is marked by the loss of transverse stability by a periodic orbit of the chaotic attractor in the invariant manifold. In the presence of the invariant manifold, there are three ways by which such a loss of transverse stability can occur: the eigenvalue of the transverse map can increase through (i) $+1$ or (ii) -1 or (iii) be complex and increase through the unit circle. These three ways generically correspond to (i) a pitchfork or transcritical bifurcation, (ii) a period-doubling bifurcation, and (iii) a Hopf bifurcation [14]. In [7] and [8] the behavior of a system undergoing a bubbling transition associated with a pitchfork and transcritical bifurcation [case (i)] was studied, and results for the average interburst time and maximum burst amplitude were derived. In [15] the stability of low period orbits and the transition to bubbling due to the three generic types of bifurcations were observed, and conditions determining whether the transition is hard or soft were derived for a system of coupled Rössler attractors. The bifurcation scenarios in case (i) were explored further in [16,17], while period-doubling induced bubbling [case (ii)] was observed in [18,19]. In [17] and [19], the effect of both fixed and random perturbations on the average interburst time and maximum burst amplitude was considered. Our results for case (ii) in Sec. IV are consistent with the scaling results in [17,19] for average interburst time as a function of perturbation size; however, we focus instead on the dependence on the normal parameter and on those scaling regions for which bursting is dominated by either the normal parameter or the random term.

In our paper we present a unified treatment covering all generic types of bubbling bifurcation. The contributions of the present paper are as follows: (i) We derive theoretically the conditions for hard and soft bubbling transitions for three generic types of bubbling bifurcation in terms of the coefficients of the canonical forms; (ii) we derive theoretically the scaling of the maximum burst amplitude and average interburst time with the normal parameter, and, in the case of interburst time, the size of perturbations transverse to the invariant manifold; (iii) we verify our predicted scalings by the results of numerical experiments. We present analyses of both mismatch-induced and noise-induced bubbling, but we pay particular attention to the case of noise-induced bubbling, where we use the Fokker-Planck diffusion approximation to obtain the interburst time scaling results. Our derivations are based on model systems, where we use canonical forms of the bifurcations to represent the transverse dynamics.

As a specific example of a system that our analysis might be applied to, consider the general case of synchronization of two coupled oscillators, as described by the following system of equations:

$$\frac{d\mathbf{z}_1}{dt}=\mathbf{F}_1(\mathbf{z}_1)+k\mathbf{f}_1(\mathbf{z}_1-\mathbf{z}_2), \tag{1a}$$

$$\frac{d\mathbf{z}_2}{dt}=\mathbf{F}_2(\mathbf{z}_1)+k\mathbf{f}_2(\mathbf{z}_2-\mathbf{z}_1), \tag{1b}$$

where $\mathbf{f}_{1,2}$ and $\mathbf{F}_{1,2}$ are smooth functions, $\mathbf{f}_1(\mathbf{0})=\mathbf{f}_2(\mathbf{0})=\mathbf{0}$, and k is a coupling constant. For this situation k is the normal parameter in the system. First consider the case where the oscillators are identical, $\mathbf{F}_1(\mathbf{z})=\mathbf{F}_2(\mathbf{z})=\mathbf{F}(\mathbf{z})$. The synchronized state $\mathbf{z}_1=\mathbf{z}_2$ represents an invariant surface embedded in the full $(\mathbf{z}_1,\mathbf{z}_2)$ phase space. Let $\mathbf{x}=(\mathbf{z}_1+\mathbf{z}_2)/2$ and $\mathbf{y}=(\mathbf{z}_1-\mathbf{z}_2)/2$. In these coordinates $(\mathbf{x},\mathbf{y})$ the dynamics in $\mathbf{x}$ with $\mathbf{y}=\mathbf{0}$ represents the dynamics along the invariant manifold. We ask, what is the effect of small perturbations to this system caused by noise or mismatch on the dynamics in the $\mathbf{y}$ direction (i.e., transverse to the invariant manifold)? In particular, what is the effect of a small noise of order r added to the right-hand sides of Eqs. (1) or of a small deviation such that the two oscillators are not identical (mismatch), $\|\mathbf{F}_1-\mathbf{F}_2\|\sim q\ll 1$? These perturbations will typically destroy the invariance of the invariant manifold $\mathbf{z}_1=\mathbf{z}_2$. In what follows we consider discrete time systems, possibly obtained via a surface of section from a continuous time system [e.g., Eqs. (1)]. If the synchronized state $\mathbf{z}_1=\mathbf{z}_2$ without noise or mismatch is chaotic, we can model the dynamics using the following model systems.

II. MODEL SYSTEMS

To simplify our analysis we assume that the chaotic dynamics on the invariant manifold is given by $x_{n+1}=2x_n \bmod 1$ and that the periodic orbit that becomes transversely unstable at the bubbling bifurcation is the fixed point $x=0$. More generally, the bifurcation may occur at a higher period orbit, but this orbit will typically have low period [12]. Our results below depend on the dynamics within and transverse to the invariant manifold in the following ways. Within the invariant manifold, the results depend only on the largest Lyapunov exponent of the bifurcating orbit, which we denote by $h_{\|}$. Transverse to the invariant manifold, our results depend on the local dynamics in the ''center manifold'' corresponding to the eigenvalue(s) on the unit circle at the bifurcation, which we represent by a complex variable z in the case of a Hopf bifurcation and by a real variable y for the other bifurcations. We include only the quadratic and cubic terms in y and z that are necessary to determine the *normal form* for the bifurcation—that is, to describe the bifurcation to the lowest order. For details on center manifolds and normal forms, see [20].

Model for pitchfork and transcritical bifurcations. For the case of a transverse pitchfork or transcritical bifurcation we consider a model system of the form [8]:

$$x_{n+1}=2x_n \mod 1, \tag{2a}$$

$$y_{n+1}=[\cos(2\pi x_n)+p]y_n+ay_n^{\sigma}+q+r\nu_n \quad \text{for } |y|<1, \tag{2b}$$

where x_n and y_n are real, p is the bifurcation parameter with $p>0$ ($p<0$) above (below) the bubbling transition, and q is the mismatch parameter. The $r\nu_n$ term represents noise in the system with magnitude $r>0$. We assume that ν_n are random numbers uniformly distributed on $[-1,1]$. The term ay^σ with $\sigma=2$ or 3 in Eq. (2b) represents the lowest order y nonlinearity of the system at the fixed point $x=0$. We assume that $|p|\ll 1$, $|q|\ll 1$, and $|r|\ll 1$ but $|a|=O(1)$. The dynamics in x models the chaotic dynamics in the invariant manifold and the dynamics in y models the dynamics transverse to the invariant manifold. In this and the following models the equation for the y dynamics models the local evolution of the system close to the invariant manifold. For $|y|>1$, it is presumed that Eq. (2b) does not apply and that there is a confining nonlinearity that sends the orbit back to the region $|y|<1$ (in particular, there is no attractor in $|y|>1$). Considering $q=0$ and $r=0$, the linearized y dynamics at the fixed point $x=0$ is governed by $y_{n+1}=(1+p)y_n$; thus, as p increases through zero, dy_{n+1}/dy_n increases through $+1$, corresponding to a pitchfork or transcritical bifurcation in the transverse dynamics at the $x=0$ fixed point. Symmetric coupling ($\mathbf{f}_1=\mathbf{f}_2$) in Eq. (1) is modeled by $\sigma=3$, and asymmetric coupling ($\mathbf{f}_1\neq\mathbf{f}_2$) is modeled by $\sigma=2$. For the symmetric case, the symmetry $y\to -y$ rules out the possibility of a y^2 term in Eq. (2b). The term q represents a small mismatch $\mathbf{F}_1-\mathbf{F}_2$. In the absence of noise and mismatch we have an invariant line $y=0$, on which there exists a chaotic invariant set generated by Eq. (1a). The stability of this line is governed by the coefficient of y_n in the first term on the right hand side of Eq. (3b). Since $\cos(2\pi x_n)$ is maximum at $x=0$, the period-1 orbit at $(x,y)=(0,0)$ with $q=0$ and $r=0$ becomes transversely unstable as p increases through zero, and the corresponding bifurcation is a transcritical bifurcation if $\sigma=2$ (asymmetric coupling) or a pitchfork bifurcation if $\sigma=3$ (symmetric coupling). In terms of Eqs. (1), p is analogous to (k_c-k), where k_c is the critical bubbling value of the coupling strength k. We refer to $p=0$ as the critical parameter value. Because the local structure of a pitchfork or transcritical bifurcation (e.g., subcritical or supercritical) is determined by the lowest order nonzero nonlinear term, we neglect all terms of order higher than y^σ. Note that the chaos in the invariant manifold ($y=0$) is unaffected by p [Eq. (2a) is independent of p].

Model for period-doubling bifurcations. For the period-doubling case we consider a model system of the form

$$x_{n+1}=2x_n \mod 1, \tag{3a}$$

$$y_{n+1}=-[\cos(2\pi x_n)+p]y_n+ay_n^2+by_n^3+q+r\nu_n, \quad \text{for } |y|<1, \tag{3b}$$

where x_n and y_n are real, p is the bifurcation parameter with $p>0$ ($p<0$) above (below) the bubbling transition, and a, b, q, and $r>0$ are parameters of the system whose values define the type of transition occurring as p goes through 0. Again we assume that $|p|,|q|,|r|\ll 1$ and $\max(|a|,|b|)=O(1)$. The ν_n are random numbers uniformly distributed on $[-1,1]$. Considering $q=0$ and $r=0$, the linearized y dynamics at the $x=0$ fixed point of Eq. (3a) is $y_{n+1}=-(1+p)y_n$ which becomes unstable as p increases through zero with dy_{n+1}/dy_n decreasing through -1, corresponding to a period-doubling bifurcation. In the case of coupled oscillators (1) with symmetric coupling ($\mathbf{f}_1=\mathbf{f}_2$), $a=0$, but with asymmetric coupling ($\mathbf{f}_1\neq\mathbf{f}_2$), both quadratic and cubic terms may be present. Because the local structure of a period-doubling bifurcation is determined by the terms of order up to 3, we neglect all terms of order higher than y^3, and, since both the quadratic and cubic terms are important, we do not treat the cases of symmetric and asymmetric coupling separately.

Model for Hopf bifurcations. In the case where the transverse bifurcation of the periodic orbit is a Hopf bifurcation, we employ the following model:

$$x_{n+1}=2x_n \mod 1, \tag{4a}$$

$$z_{n+1}=[\cos(2\pi x_n)+p]e^{i\theta}z_n+az_n^2+bz_nz_n^*+c(z_n^*)^2+d|z_n|^2z_n+q+r\nu_n \quad \text{for } |z|<1, \tag{4b}$$

where z_n is complex and z_n^* is the complex conjugate of z_n. As in the previous cases, p and r are small real parameters. The quantities a, b, c, d, q, and r are complex parameters of the system with $|q|,|r|\ll 1$ and $|\max(a,b,c,d)|=O(1)$. The ν_n are complex random numbers uniformly distributed within the unit circle. In this model complex z models the two-dimensional dynamics transverse to the invariant manifold, while the variable x models the dynamics along the invariant manifold. For $q=0$ and $r=0$, the quantity dz_{n+1}/dz_n evaluated at the fixed point $x=0$ has its magnitude increase through unity as p increases through zero. For $\theta/2\pi$ irrational this corresponds to a Hopf bifurcation. This model includes the above mentioned pitchfork or transcritical and period-doubling bubbling bifurcations as special cases with $\theta=0$ being the pitchfork or transcritical case and $\theta=\pi$ being the period-doubling case. Although it is possible to get all results for period-doubling and pitchfork or transcritical bifurcations from the model (4), we will use the models (2) and (3) for these special cases to simplify the analysis. The mismatch parameter q again breaks the invariance of the line $z=0+0i$. We included all possible terms quadratic in z. In previous work on the Hopf bifurcation it has been shown that out of all possible terms cubic in z only the term proportional to $|z_n|^2z_n$ is relevant to the local structure of the bifurcation [22].

The results we obtain for models (2), (3), and (4) are given in Tables I–III. We treat the cases of mismatch ($q\neq 0$) and noise ($r\neq 0$) separately; when both q and r are nonzero, the average interburst time will scale as the smaller of the two expressions given. We claim that these results can be applied to any generic situation exhibiting a bubbling transition. For the case of the pitchfork or transcritical bifurcation this claim has been confirmed experimentally (see [8]).

TABLE I. Summary of results for the pitchfork and transcritical bifurcations using the model system (2), with $D=(1/2)r^2\,\mathrm{Var}(\nu)$.

	Symmetric coupling ($\sigma=3$)	Asymmetric coupling ($\sigma=2$)
Condition for hard transition	$a>0$	$qa>0$ or $r\neq 0$
Condition for soft transition	$a<0$	$qa<0$ and $r=0$
Maximum burst amplitude (soft transition)	$\Delta\simeq(p/\lvert a\rvert)^{1/2}$ for $\max(\lvert q\rvert,\lvert r\rvert)^{2/3}\ll p\ll 1$	$\Delta\simeq p/\lvert a\rvert$ for $q^{1/2}\ll p\ll 1$
Average interburst time (mismatch)	$\ln\tau\sim(h_\parallel/p)\ln[p^{3/2}/\lvert aq^2\rvert^{1/2}]$ for $\lvert q\rvert^{2/3}\ll p\ll 1$	$\ln\tau\sim(h_\parallel/p)\ln[p^2/\lvert aq\rvert]$ for $\lvert q\rvert^{1/2}\ll p\ll 1$
Average interburst time (noise)	$\ln\tau\sim(h_\parallel/2p)\ln[p^2/\lvert aD\rvert]$ for $r^{2/3}\ll p\ll 1$	$\ln\tau\sim(h_\parallel/2p)\ln[p^3/(a^2D)]$ for $r^{1/2}\ll p\ll 1$
	$\ln\tau\sim h_\parallel^{1/2}\lvert aD\rvert^{-1/3}-\frac{1}{4}p(aD)^{-2/3}$	$\ln\tau\sim h_\parallel^{1/2}(a^2D)^{1/4}-\frac{1}{4}p(a^2D)^{-1/2}$
	for $p\ll r^{2/3}\ll 1$	for $p\ll r^{1/2}\ll 1$

III. PITCHFORK AND TRANSCRITICAL BIFURCATIONS

A. Maximum burst amplitude and stability

In this subsection we review the derivation of the theoretical result for the maximum burst amplitude for the case of a pitchfork or transcritical bubbling bifurcation in the map (2). We derive the results for the noiseless case $r=0$ first. This derivation serves as a model for the treatments of the period-doubling and Hopf cases, and closely follows [7,8]. In the case of symmetric coupling ($\sigma=3$) we will show that we have a soft bubbling transition if $a<0$ and a hard bubbling transition if $a>0$. In the case of asymmetric coupling ($\sigma=2$), we will show that $qa>0$ corresponds to a hard transition, and $qa<0$ corresponds to a soft transition.

For small positive p, the factor $[p+\cos(2\pi x_n)]$ is greater than 1 only in a small region near the fixed point $x=0$ of Eq. (1a) (since x is taken modulo 1, we consider values of x near 1 to be near 0). Thus a burst can only be initiated when the chaotic x orbit comes near enough to $x=0$ that it remains there long enough for y to burst. The burst ends when x moves away from the fixed point. In order to compute the maximum possible burst amplitude, we first consider the dynamics when $x=0$. Then y satisfies the relation

$$y_{n+1}-y_n=py_n+ay_n^\sigma+q. \tag{5}$$

Assume for definiteness that $q>0$. Then, in the case of a soft transition ($a<0$), if $x=0$ then y increases but is bounded from above by the positive solution of

$$p\Delta+a\Delta^\sigma+q=0. \tag{6}$$

Since the maximum value that y can reach is Δ, this value represents the maximum burst amplitude for all trajectories that start near $y=0$. Since $a\Delta^\sigma$ is the only negative term on the left-hand side of Eq. (6), the solution for Δ can be estimated by $\Delta^\sigma\simeq\max(p\Delta/\lvert a\rvert,\lvert q/a\rvert)$ which yields

$$\Delta\simeq\max((p/\lvert a\rvert)^{1/(\sigma-1)},\lvert q/a\rvert^{1/\sigma}). \tag{7}$$

(In this and further equations we use $\simeq$ to denote "approximately equal" and $\sim$ to denote "equal up to a constant.") In particular, when $p\gg q^{(\sigma-1)/\sigma}$, we have $\Delta\simeq\lvert p/a\rvert^{1/(\sigma-1)}$.

TABLE II. Summary of results for the period-doubling bifurcation using the model system (3). We use the notation $\hat{p}=p-aq$ and $D=(1/2)r^2\,\mathrm{Var}(\nu)$.

Condition for hard transition	$a^2+b<0$
Condition for soft transition	$a^2+b>0$
Maximum burst amplitude (soft transition)	$\Delta\simeq\sqrt{\hat{p}/(a^2+b)}$ for $\max(\lvert q\rvert^2,r^{2/3})\ll\hat{p}\ll 1$
Average interburst time (mismatch)	$\ln\tau\sim(h_\parallel/2\hat{p})\ln[\hat{p}/(\lvert a^2+b\rvert q^2)]$ for $\lvert q\rvert^2\ll\hat{p}\ll 1$
Average interburst time (noise)	$\ln\tau\sim(h_\parallel/2p)\ln[p^2/(\lvert a^2+b\rvert D)]$ for $r^{2/3}\ll p\ll 1$
	$\ln\tau\sim h_\parallel^{1/2}[(a^2+b)D]^{-1/3}-\frac{1}{4}p[(a^2+b)D]^{-2/3}$ for $p\ll r^{2/3}\ll 1$

TABLE III. Summary of results for the Hopf bifurcation [f_1 is defined in Eq. (42), and $D=(1/2)r^2\,\mathrm{Var}(\nu)$].

Condition for hard transition	$\mathrm{Re}\{[(1-2e^{i\theta})e^{-2i\theta}/(1-e^{i\theta})]ab\}+(1/2)bb^*+cc^*$ $-\mathrm{Re}(de^{-i\theta})<0$
Condition for soft transition	$\mathrm{Re}\{[(1-2e^{i\theta})e^{-2i\theta}/1-e^{i\theta}]ab\}+(1/2)bb^*+cc^*$ $-\mathrm{Re}(de^{-i\theta})>0$
Maximum burst amplitude (soft transition)	$\Delta\simeq\sqrt{p/f_1}$ for $\max(\lvert q\rvert,r^{2/3})\ll p\ll 1$
Average interburst time (mismatch)	$\ln\tau\sim(h_\parallel/2p)\ln\lvert p(1-e^{i\theta})^2/\lvert f_1 q\rvert^2\rvert$ for $\lvert q\rvert\ll p\ll 1$
Average interburst time (noise)	$\ln\tau=(h_\parallel/2p)\ln[p^2/\lvert f_1 D\rvert)$ for $r^{2/3}\ll p\ll 1$ $\ln\tau=h_\parallel^{1/2}(f_1D)^{-1/3}-\frac{1}{4}p(f_1D)^{-2/3}$ for $p\ll r^{2/3}\ll 1$

When $q<0$, a soft transition will occur if and only if Eq. (6) has a negative root Δ. Thus if $\sigma=2$ we need $a>0$ for a soft transition, while if $\sigma=3$ we need $a<0$. In these cases, the magnitude of the negative root Δ is given by the right side of Eq. (7). In the case of noise, for asymmetric coupling ($\sigma=2$) the transition is always hard; because the noise can take either sign, there will be both large and small bursts. For symmetric coupling ($\sigma=3$), we still have a soft transition if $a<0$ and a hard transition if $a>0$. In the case of a soft transition, by arguments similar to the one above, we have $\Delta\simeq(p/\lvert a\rvert)^{1/(\sigma-1)}$ when $r^{2/3}\ll p\ll 1$.

B. Average interburst time: Mismatch

In what follows we derive results for the average interburst time for soft and hard bubbling transitions. We first consider the effect of mismatch in the noiseless case $r=0$. The analysis in the previous section shows that the nonlinear term ay^σ is insignificant when $\lvert y\rvert\ll y_c\sim\max((p/\lvert a\rvert)^{1/(\sigma-1)},(q/\lvert a\rvert)^{1/\sigma})$, while when y grows close to y_c, the nonlinear term will either confine the burst (soft transition) or rapidly accelerate the orbit to $y=O(1)$ (hard transition). Either way, we can estimate the interburst time as the time for $\lvert y\rvert$ to reach y_c in the absence of the nonlinear term.

Assuming that x stays at its fixed point $x=0$, the nth iterate y_n for $n>0$ in the absence of the nonlinearity can be written as

$$y_n=\sum_{i=0}^{n-1}(1+p)^i q=\frac{[(1+p)^n-1]q}{p}. \tag{8}$$

Hence we can compute the time $\overline{n}$ for an initial point $(x_0,y_0)=(0,0)$ to reach y_c by setting $y_{\overline{n}}=y_c$ which yields

$$\overline{n}\sim\frac{1}{p}\ln\left(\frac{py_c}{\lvert q\rvert}\right). \tag{9}$$

This expression is valid for $py_c\gg q$, which corresponds to the case $p\gg q^{(\sigma-1)/\sigma}$ and $y_c\sim(p/\lvert a\rvert)^{1/(\sigma-1)}$. To estimate the average interburst time τ we note that, in order to initiate a burst, an orbit must come within ε of $x=0$ where ε is sufficiently small that the orbit remains near $x=0$ for at least $\overline{n}$ iterates. Since the invariant density generated by Eq. (3) is uniform in x, we have that the average time τ between bursts is given by $\tau^{-1}=\varepsilon$. We express ε in terms of $\overline{n}$ as follows. For small initial x_0 near $x=0$, the subsequent iterates grow exponentially as $x_0\exp(h_\parallel n)$ where $h_\parallel=\ln 2$ is the Lyapunov exponent of Eq. (1a). Requiring that $\varepsilon\exp(h_\parallel\overline{n})\lesssim\delta$, where $\delta<1$ is $O(1)$, we obtain the desired estimate of ε and hence of the average interburst time in terms of $\overline{n}$:

$$\ln\tau\sim\ln\varepsilon^{-1}=h_\parallel\overline{n}. \tag{10}$$

Substituting $\overline{n}$ from Eq. (9) into Eq. (10) we obtain the result for the scaling of $\ln\tau$,

$$\ln\tau\sim\frac{h_\parallel}{p}\ln\left(\frac{py_c}{\lvert q\rvert}\right). \tag{11}$$

This result is recorded in Table I with the appropriate value of y_c substituted.

C. Average interburst time: Noise

We now derive the scaling for the average interburst time in the presence of small bounded noise in the map (2). We isolate the effect of noise by taking $q=0$. We consider the y dynamics in this case to be a drift-diffusion problem with drift proportional to terms linear in y, i.e., py, and diffusion due to noise $r\nu_n$. We split the problem into two parts: First we consider drift-dominated bubbling corresponding to the case where the effect of the py drift is dominant in developing a burst, and then we consider noise-dominated bursting corresponding to the case where the effect of the noise term $r\nu_n$ is dominant. For both cases we will derive asymptotic upper bounds on the mean interburst time, and our final result for the interburst time will be the minimum of these two bounds. We also derive a relation between p and r that determines what kind of bursting is dominant and thus which scaling applies.

First we consider noise-dominated bursting. In this case Eq. (2b) with $x=0$ can be approximated as a random walk process with small drift. We characterize this process with two quantities: the drift per iterate py_n and the diffusion coefficient $D=(1/2)r^2\,\mathrm{Var}(\nu)$. Here $\mathrm{Var}(\nu)$ is the variance of the random variable ν_n (mean value of ν_n^2). For our numerical experiments ν_n is uniformly distributed in $[-1,1]$, in which case $\mathrm{Var}(\nu)=1/3$.

As in the previous section, we assume that there is a critical value y_c such that we can estimate the time to produce a burst as the time for $|y|$ to reach y_c in the absence of the nonlinear term ay^σ. We set y_c such that the size of the nonlinear term is equal to the typical size of the noise, $|a|y_c^\sigma \sim \sqrt{D}$. Hence we have

$$y_c \sim \left|\frac{\sqrt{D}}{a}\right|^{1/\sigma}. \tag{12}$$

By defining y_c in this manner, we ensure that the nonlinear term dominates the noise for $|y| \gg y_c$. However, it is possible that the nonlinear term becomes significant for $|y| \ll y_c$ because it behaves coherently from one iterate to the next while the noise term may not. Thus by ignoring the nonlinear term for $|y|<y_c$ we may be overestimating the interburst time. However, our estimate remains an upper bound on the interburst time, and our simulations show that this upper bound correctly describes the actual interburst time scaling in the noise-dominated case. The reason for this is that a burst most often occurs when the noise does behave coherently; we discuss this point further in Sec. VI.

The average interburst time τ is the inverse of the probability per unit time of initiating a burst. By initiating a burst, we mean that x maps close to 0 (having not been close on the previous iteration), and that a burst will happen during the time x remains close to 0. In the previous section, we could say exactly how many iterations ($\overline{n}$) x needed to remain close to 0 in order for a burst to occur, but in the noise-dominated case we cannot. Instead, we proceed as follows. Let $Q(n)$ be the probability that $|y|$ has remained in the range $|y|<y_c$ up to time n. The probability that $|y|$ exceeds y_c for some time at or before time n is $1-Q(n)$. As in the previous section, the probability that x will map close enough to 0 to stay there for at least n iterations is proportional to $e^{-h_\parallel n}$. Thus the probability that x remains close to zero for exactly n iterations is proportional to $e^{-h_\parallel n}-e^{-h_\parallel (n+1)}$. Hence $1/\tau$, the probability per unit time of initiating a burst, satisfies

$$\frac{1}{\tau} \simeq \sum_{n=0}^{\infty} \{(e^{-h_\parallel n}-e^{-h_\parallel (n+1)})[1-Q(n)]\}. \tag{13}$$

To estimate Eq. (13) we utilize a continuous time approximation for the y dynamics, with the continuous variable t replacing n. Equation (13) becomes

$$\frac{1}{\tau} \simeq h_\parallel \int_0^\infty e^{-h_\parallel t}[1-Q(t)]dt = 1-h_\parallel \int_0^\infty e^{-h_\parallel t} Q(t)dt. \tag{14}$$

The continuous time approximation of Eq. (13) requires that $h_\parallel$ be small. We note, however, that Eq. (14) is valid as an order of magnitude estimate even when $h_\parallel$ is of order 1. Since $\tau \gg 1$, and since we will use Eq. (14) only to estimate the logarithm of τ, an order of magnitude estimate is sufficient. To estimate $Q(t)$, we consider the time evolution of the probability distribution function for y, $P(y,t)$ for the situation in which an orbit starts at $y=0$ at time $t=0$ and is considered to burst when $|y|$ exceeds y_c. Accordingly, we assume that $P(y,0)=\delta(y)$ and that $P(y,t)=0$ for $|y| \geqslant y_c$, so that $P(y,t)$ for $|y|<y_c$ represents the probability distribution function for trajectories that have not yet reached $|y|=y_c$ at time t. Thus

$$Q(t) = \int_{-y_c}^{y_c} P(y,t)dy \tag{15}$$

and

$$\ln \tau \sim -\ln\left\{1-h_\parallel \int_{-y_c}^{y_c}\int_0^\infty e^{-h_\parallel t} P(y,t)dt\,dy\right\}. \tag{16}$$

We obtain the probability distribution function $P(y,t)$ using the Fokker-Planck diffusion approximation. Ignoring the nonlinear terms ay^σ, the evolution of the probability distribution function $P(y,t)$ is given by the solution of the following drift-diffusion equation:

$$D\frac{\partial^2 P}{\partial y^2} = \frac{\partial P}{\partial t} + \frac{\partial}{\partial y}(pyP), \tag{17}$$

where py and D are the above mentioned drift velocity and average diffusion per iterate parameters. Recall that the initial condition is $P(y,0)=\delta(y)$ and the boundary conditions are $P(\pm y_c,t)=0$. We solve this equation by first performing a Laplace transform with respect to the time variable t,

$$\overline{P}(y,s) = \int_0^\infty e^{-st} P(y,t)dt. \tag{18}$$

Note that this integral is the same as the integration over dt on the right-hand side of Eq. (16) with s replaced by $h_\parallel$. Thus

$$\ln \tau \sim -\ln\left\{1-h_\parallel \int_{-y_c}^{y_c} \overline{P}(y,h_\parallel)dy\right\}. \tag{19}$$

The differential equation for $\overline{P}(y,s)$ is

$$D\frac{\partial^2 \overline{P}}{\partial y^2} - py\frac{\partial \overline{P}}{\partial y} - (p+s)\overline{P} = -\delta(y), \tag{20}$$

with boundary conditions $\overline{P}(\pm y_c,s)=0$. The exact solution of this equation satisfying the boundary conditions can be expressed in terms of parabolic cylinder functions [21], and is rather cumbersome. For small p we have developed a perturbation expansion approach that gives the lowest order in p behavior. We first find the solution to Eq. (20) for $p=0$ and call it $\overline{P}_0(y,s)$. Then we represent $\overline{P}(y,s)$ in the form

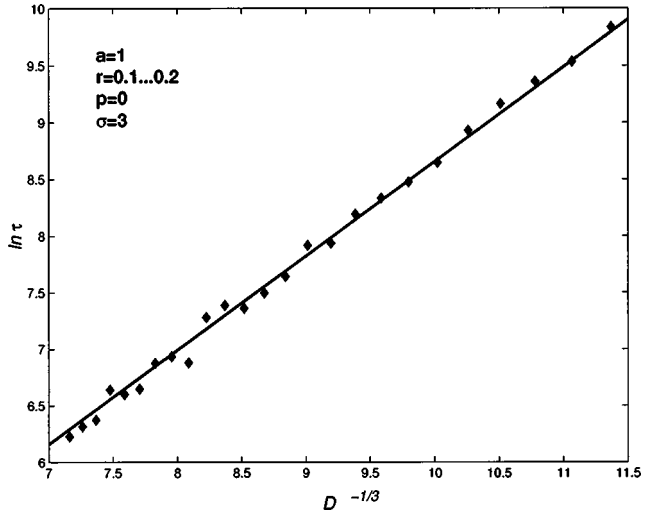

FIG. 1. This plot shows $\ln \tau$ vs $D^{-1/3}$ for bubbling induced by a pitchfork bifurcation with noise in noise-dominated case, $p \ll r^{2/3} \ll 1$. D is the diffusion coefficient, $D=(1/2)r^2\,\mathrm{Var}(\nu)$. Parameter values are $a=1$, $p=0$, $\sigma=3$, and $r=0.1,\ldots,0.2$. The experimental data are plotted as diamonds. The solid curve has the slope $\sqrt{h_\parallel}=\sqrt{\ln 2}$ predicted by scaling given in Table I.

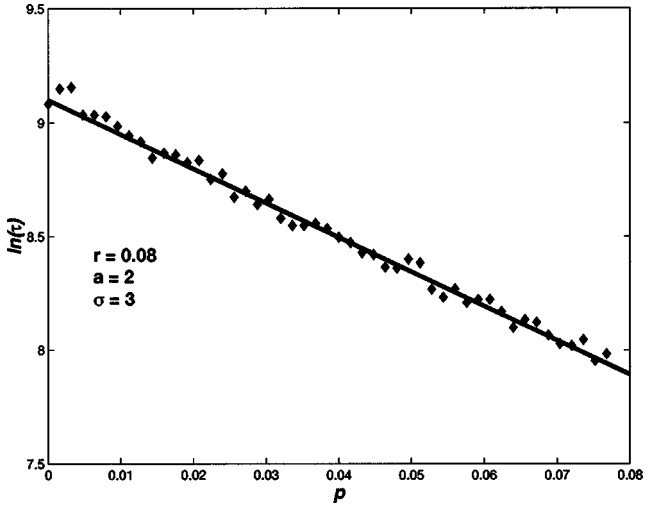

FIG. 2. This plot shows $\ln \tau$ vs p for bubbling induced by pitchfork bifurcation with noise in the noise-dominated case, $p \ll r^{2/3} \ll 1$. Parameter values are $a=2$, $r=0.08$, and $\sigma=3$. The experimental data are plotted as diamonds. The solid curve has slope -15.1 predicted by scaling given in Table I.

$\overline{P}(y,s)=\overline{P}_0(y,s)+p\overline{P}_1(y,s)+O(p^2)$, substitute this form into Eq. (20) and solve for $\overline{P}_1(y,s)$ subject to $\overline{P}_1(\pm y_c,s)=0$. Thus we obtain the first order in p correction to the solution (see the Appendix). Writing τ in terms of $\overline{P}(y,s)$ we obtain

$$\ln \tau \sim -\ln\left\{1-h_\parallel \int_{-y_c}^{y_c} [\overline{P}_0(y,h_\parallel)+p\overline{P}_1(y,h_\parallel)]dy\right\}+O(1). \tag{21}$$

Performing the integral above, and making the appropriate approximations (see the Appendix), we obtain the scaling of $\ln \tau$ with p and D:

$$\ln \tau \sim y_c\sqrt{h_\parallel/D}-\frac{py_c^2}{4D}. \tag{22}$$

This scaling is valid as long as the second term is small compared to the first one; that is, when $p^{\sigma/(\sigma-1)}/|r| \ll 1$. Upon substitution of the expression (12) for y_c into Eq. (22), we obtain our final expression for the scaling of $\ln \tau$,

$$\ln \tau \sim \sqrt{h_\parallel/D}\left|\frac{\sqrt{D}}{a}\right|^{1/\sigma}-\frac{p}{4D}\left|\frac{\sqrt{D}}{a}\right|^{2/\sigma}. \tag{23}$$

This equation is also given in Table I.

To numerically test the scaling results, we iterated map (2) starting at $y=0$ and a typical (irrational) value of x with ν_n distributed uniformly on $[-1,1]$, and measured the average interburst time for different values of the parameters p and r. Figure 1 compares the derived scaling (solid line) with the results from the numerical experiment (diamonds), where $p=0$ and r is varied. In Fig. 2, we vary p, keeping r fixed.

We now consider drift-dominated bursting. In this case, we again claim that a burst occurs when y becomes greater than a critical value y_c beyond which the nonlinear term dominates. As an upper bound for the critical value y_c we use the same value for the burst threshold as we used in the case of mismatch, i.e., $y_c=(p/|a|)^{(\sigma-1)^{-1}}$. If $y \sim y_c$ the nonlinear term either confines the orbit (for $\sigma=3$ and $a<0$), or else rapidly accelerates the orbit to $y \sim O(1)$. As in the mismatch case we first estimate the average number of iterates required for y to reach y_c starting at a value $y_0=0$, ignoring the nonlinear term and assuming that x stays at 0 (unlike for noise-dominated bursting, the number of iterates does not depend strongly on whether the noise behaves coherently). The nth iterate then can be written as

$$y_n=r\sum_{i=0}^{n-1}(1+p)^i\nu_i. \tag{24}$$

Since ν_i are random variables with mean zero, we deduce that

$$\mathrm{Var}(y_n)=\frac{2[(1+p)^{2n}-1]}{p(2+p)}D,$$

where $D=(1/2)r^2\mathrm{Var}(\nu)$ is the previously defined average diffusion per iterate. For $p \ll 1$, we can simplify the expression for the variance $\mathrm{Var}(y_n) \simeq (D/p)[(1+p)^{2n}-1]$. Now we set the burst condition to $\mathrm{Var}(y_{\bar{n}})=y_c^2$, where $\bar{n}$ is the average number of iterates of the map required on average for y_n to become equal to or greater than y_c,

$$\frac{D}{p}[(1+p)^{2\bar{n}}-1] \simeq y_c^2. \tag{25}$$

Solving the above equation for $\bar{n}$, and dropping higher order p and D terms, we obtain

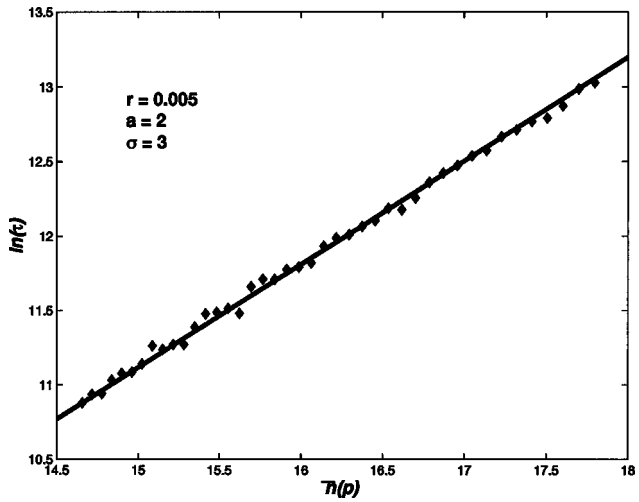

FIG. 3. This plot shows $\ln\tau$ vs $\bar{n}(p)$, where $\bar{n}(p)$ is given by Eq. (26), for bubbling induced by a pitchfork bifurcation with noise in the drift-dominated case, $r^{2/3}\ll p\ll 1$. Parameter values are $a=2$, $\sigma=3$, and $r=0.005$. The experimental data are plotted as diamonds. The solid curve has slope $\ln 2$ predicted by scaling given in Table I.

$$\bar{n}\simeq\frac{1}{2p}\ln\left(\frac{py_c^2}{D}\right). \tag{26}$$

Notice that, if the noise behaved coherently (say $\nu_n=1$ for all n), the result for $\bar{n}$ would differ only in that p would be replaced by p^2 inside the logarithm [one can see this by replacing $|q|$ with r in Eq. (9)]. Using $\ln\tau\sim h_\parallel\bar{n}$, we obtain

$$\ln\tau\sim\frac{h_\parallel}{2p}\ln\left(\frac{py_c^2}{D}\right). \tag{27}$$

This is the final scaling result given in the Table I.

We have numerically tested our theoretical result for drift-dominated bubbling by iterating the map (2) starting at $y=0$ and a typical (irrational) value of x with ν_n distributed uniformly on $[-1,1]$, and measuring the average interburst time. The parameter p was varied with the other parameter values set at $a=2$, $\sigma=3$, and $r=0.005$. In Fig. 3 we plot $\ln\tau$ from the numerical experiments vs $\bar{n}(p)$ given by Eq. (26). The results of the numerical experiments are shown as diamonds. The solid curve has a slope of $h_\parallel=\ln 2$ predicted by the scaling given in Table I.

Now we consider the condition on p and r that determines what kind of bursting prevails, and hence which scaling applies. To do that, we set the two relations Eq. (23) and Eq. (27) equal in the lowest significant order:

$$\sqrt{h_\parallel/D}\left|\frac{\sqrt{D}}{a}\right|^{1/\sigma}\simeq\frac{h_\parallel}{p}. \tag{28}$$

We arrive at the conclusion that the two scalings agree when $p^{\sigma/(\sigma-1)}/|r|\simeq O(1)$. Thus noise-dominated bubbling prevails when $p^{\sigma/(\sigma-1)}/|r|\ll 1$ and the drift-dominated bubbling prevails if $p^{\sigma/(\sigma-1)}/|r|\gg 1$. This result is consistent with the order-of-magnitude estimate presented in Sec. VI.

IV. PERIOD-DOUBLING BIFURCATION

A. Maximum burst amplitude and stability

In this section we present a derivation of theoretical results and results of numerical experiments for the period-doubling bifurcation induced bubbling transition. We start with the case of no noise: $r=0$ in our model system (3). Consider an orbit starting at $(x,y)=(0,0)$ for the map (2). Note that (0, 0) is a fixed point of the map for $q=0$. The subsequent iterates obey the relation

$$y_{n+2}-y_n=2(p-aq)y_n-2(a^2+b)y_n^3-(p-aq)q+O(py^2,p^2y,q^2y,qy^2,q^3,y^4,pqy). \tag{29}$$

Making the change of variables $\hat{p}=p-aq$, we have

$$y_{n+2}-y_n=2\hat{p}y_n-2(a^2+b)y_n^3-\hat{p}q+O(\hat{p}y^2,\hat{p}^2y,q^2y,q^3,qy^2,y^4,\hat{p}qy). \tag{30}$$

Of course, if $p\gg|aq|$, then $\hat{p}\simeq p$, but for smaller values of p the distinction between $\hat{p}$ and p will be significant. We proceed by analyzing Eq. (29) in the same way we treated Eq. (5). Setting $y_{n+2}-y_n=0$, we obtain the equation for the maximum burst amplitude Δ:

$$2\hat{p}\Delta-2(a^2+b)\Delta^3-\hat{p}q=0. \tag{31}$$

As for the derivation of Eq. (7) in the case $\sigma=3$, we conclude that for $a^2+b>0$,

$$\Delta\simeq\max\left\{\left(\frac{\hat{p}}{a^2+b}\right)^{1/2},\left(\frac{\hat{p}|q|}{a^2+b}\right)^{1/3}\right\}. \tag{32}$$

In particular, if $|q|^2\ll\hat{p}\ll 1$, then $\hat{p}^{1/2}\gg(\hat{p}|q|)^{1/3}$ and we have

$$\Delta\simeq\sqrt{\hat{p}/(a^2+b)}. \tag{33}$$

[A result that accounts for the effect of mismatch more accurately can be obtained by solving Eq. (31) for Δ and taking the appropriate root.] Thus for $x=0$ and $a^2+b>0$, the linear exponential increase of y (namely, $y_{n+2}-y_n\simeq 2\hat{p}y_n$) is eventually arrested by nonlinearity, and y reaches a maximum, $y=\Delta$, that is small, $O(\hat{p}^{1/2})$, for small $\hat{p}$, corresponding to a soft transition. For $a^2+b<0$, Δ does not exist, and, when $|y|\sim|\hat{p}/(a^2+b)|^{1/2}$ the nonlinearity accelerates the growth of y, leading to a hard transition.

We now obtain the conditions on the parameters that will determine whether the transition is soft or hard. The type of transition is determined by the sign of the expression under the square root in the denominator of Eq. (33), positive corresponding to a soft transition and negative corresponding to a hard transition. Thus we have that the transition is hard if $a^2+b<0$ and soft if $a^2+b>0$. We have tested the above results in numerical experiments on Eq. (3). For $b=-4$ the transition is hard if $-2<a<2$. Figure 4(a) illustrates the soft transition if we iterate Eq. (3) starting at $(x_0,y_0)=(0,0)$. The

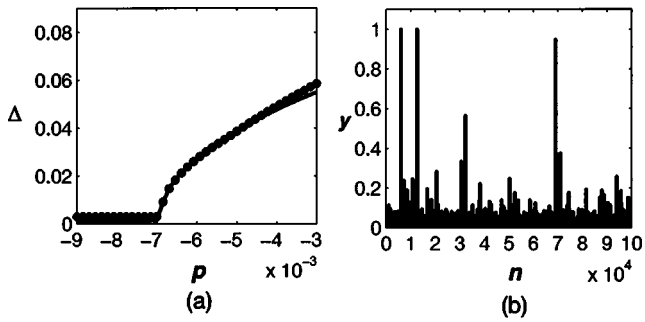

FIG. 4. Plot (a) shows the maximum burst amplitude Δ vs p for the soft transition in period-doubling induced bubbling, map (3). The experimental data are plotted as dots. The solid curve is the theoretical result from Eq. (33). Plot (b) shows the bursting time series for hard transition at $p=0.27$. Parameter values are $q=0.003$, $a=-1.9$ (a), $a=-2.3$, (b) and $b=-4$.

data from numerical experiments is plotted as dots. Figure 4(b) shows a bursting time series for a hard bubbling transition.

In the case of noise, we have a soft transition if $(a^2+b)>0$ and a hard transition if $(a^2+b)<0$. In the case of a soft transition, by arguments similar to the one above, we have $\Delta \simeq \sqrt{\hat{p}/(a^2+b)}$ when $r^{2/3} \ll p \ll 1$.

B. Average interburst time: Mismatch

To begin the analysis, we first note from Eq. (3) that the average magnitude of y between bursts is of order q. We again consider the second iterate of the map (3b), for $x=0$ with terms of higher order in p and q dropped, resulting in Eq. (29).

Equation (30) shows that in the case of a soft transition the nonlinearity limits the increase of $|y|$ at the value of $\sqrt{\hat{p}/|a^2+b|}$. Denote this value of y as the critical value y_c. In the case of a hard transition, the nonlinear terms quickly push y to $|y| \sim O(1)$ as soon as $|y|$ grows to a value of the order y_c. As mentioned earlier, at the beginning of a burst y is of order q. The term $\hat{p}q$ only determines the direction of the burst and therefore it is rather insignificant, being at most of the order of the $2\hat{p}y$ term. Thus for simplicity we ignore it and assume that, when x comes close to zero, $y \simeq q$. Then $y_n \simeq (1+2\hat{p})^{n/2} q$ and setting $y_{\overline{n}}=y_c$ we obtain the following expression for the number of iterates $\overline{n}$ required for $|y|$ to reach y_c (i.e., to initiate a burst):

$$\overline{n} \simeq \frac{1}{\hat{p}} \ln\left(\frac{y_c}{|q|}\right), \tag{34}$$

for $|q|^2 \ll \hat{p} \ll 1$. From Eqs. (9) and (34), we obtain the desired estimate for the average interburst time,

$$\ln \tau \sim h_{\|} \overline{n} = \frac{h_{\|}}{\hat{p}} \ln\left(\frac{y_c}{|q|}\right), \tag{35}$$

which is also given in Table II.

We have obtained the scaling of τ with p numerically by starting the map (3) at a random initial x and $y=0$ and measuring the average number of iterates that it took for $|y|$ to become greater than 1. For the parameters of Fig. 5 the transition is hard since $a^2+b<0$. The experimental data are plotted as diamonds. Figure 5 presents these data as $\ln \tau$ vs $\overline{n}(p)$ where $\overline{n}(p)$ is obtained from Eq. (34). The solid line has the slope of $h_{\|}=\ln 2$ predicted by Eq. (35) and is consistent with the data.

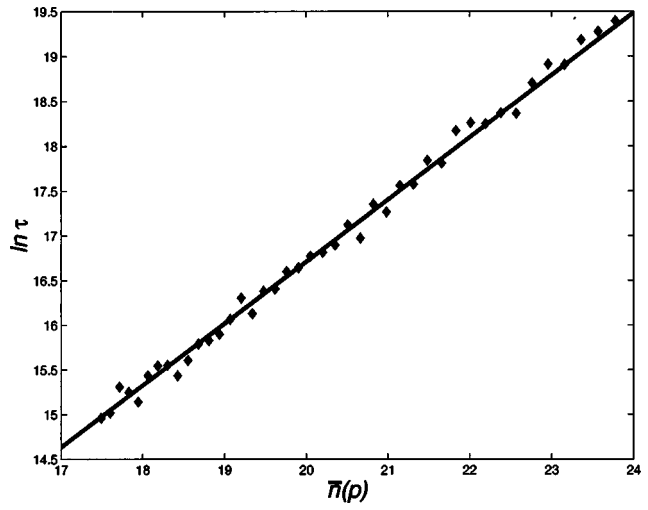

FIG. 5. This plot shows $\ln \tau$ vs $\overline{n}(p)$, where $\overline{n}(p)$ is given by Eq. (34), for bubbling induced by a period-doubling bifurcation with asymmetry for $q^2 \ll p \ll 1$. Parameter values are $a=1$, $b=-2$, $q=0.008$ with p varying from 0.14 to 0.22. The experimental data are plotted as diamonds. The solid curve has a slope of $\ln 2$ predicted by scaling given in Table II.

C. Average interburst time: Noise

In this section we deduce the expression for average interburst time for period-doubling-induced bubbling. Similar to the previous section we consider every other iterate of Eq. (3b) in the presence of noise and the absence of mismatch $(q=0)$ with x at its fixed point $x=0$:

$$y_{n+2}-y_n \simeq 2py_n - 2(a^2+b)y_n^3 + r(\nu_{n+1}-\nu_n). \tag{36}$$

We redefine the noise variable $(\nu_{n+1}-\nu_n)$ as $\hat{\nu}_n$, where $\mathrm{Var}(\hat{\nu}_n)=2\,\mathrm{Var}(\nu_n)$. With $\hat{\nu}_n$, Eq. (36) is equivalent to the case of noise in a pitchfork bifurcation $(\sigma=3)$. The variance of $\hat{\nu}_n$ is double the variance of ν_n, but since we are considering every other iterate of y_n, these two effects cancel in the computation of the average interburst time. Thus all results derived in Sec. III C apply, including the scaling ranges, if we use the derived expressions for average interburst time for $\sigma=3$ with a^2+b as the coefficient of the cubic term. The results for period-doubling bifurcation induced bubbling are summarized in Table II.

To test the scaling results we iterated map (3) starting at a typical irrational x and $y=0$ with ν_n distributed uniformly on $[-1,1]$ and measured the average interburst time for different values of p, keeping the noise magnitude r fixed. Figure 6 compares the derived scaling result with the experimental results. We plot $\ln \tau$ for different values of p keeping other parameters fixed. Numerical data are plotted as diamonds.

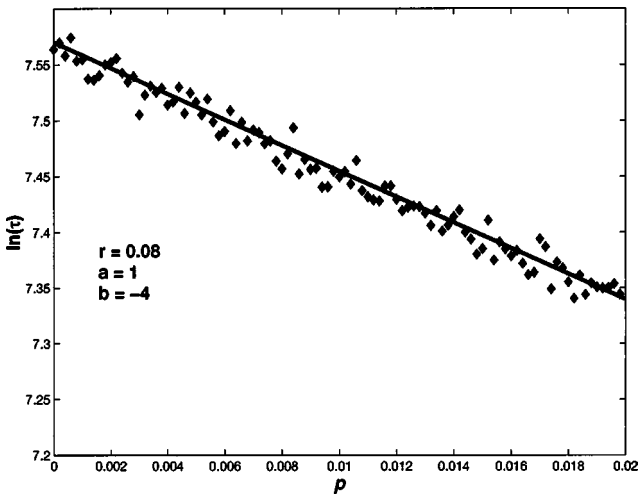

FIG. 6. This plot shows $\ln\tau$ vs p for bubbling induced by a period-doubling bifurcation with noise in the noise-dominated case, $p \ll r^{2/3} \ll 1$. Parameter values are $a=1$, $b=-4$, and $r=0.08$. The experimental data are plotted as diamonds. The solid curve has the slope -11.5 predicted by scaling given in Table II.

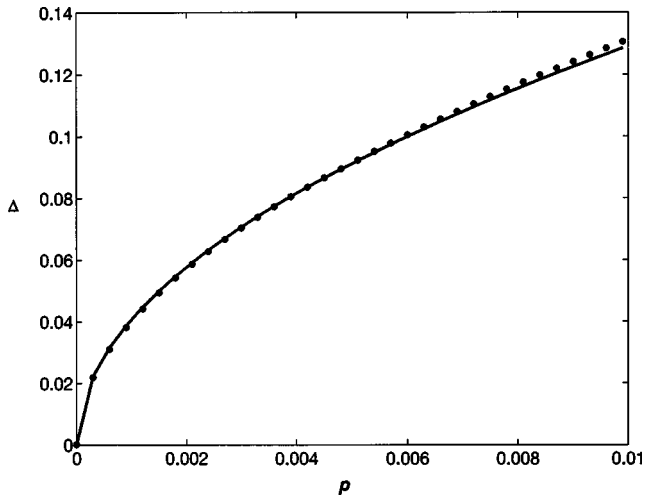

FIG. 7. This plot shows the maximum burst amplitude Δ vs p for a soft transition in Hopf-bifurcation-induced bubbling. The experimental data are plotted as dots. The solid curve is the theoretical result from Eq. (44). Parameter values are $a=0.1$, $b=0$, $c=0.1$, $d=1.0$, $\theta=\pi\sqrt{5}$, and $q=0.0001-0.0001i$.

V. HOPF BIFURCATION

A. Maximum burst amplitude and stability

Next we examine the case of a Hopf bifurcation, Eqs. (4). We consider an orbit starting at $(x,z)=(0,0+0i)$, and take $p=0$ (i.e., we consider the map at the critical bifurcation point). For the validity of the analysis below we assume that the angle θ in the exponent in front of the linear coefficient is not equal to certain special values: 0, $\pm\pi/2$, $\pm 2\pi/5$, $\pm 2\pi/3$, and $\pm\pi$. The cases $\theta=0$ and $\pm\pi$ correspond to pitchfork or transcritical and period-doubling bifurcations and have already been considered in Secs. III and IV. The other nonallowed angles $(\pm\pi/2, \pm 2\pi/5, \pm 2\pi/3)$ correspond to nongeneric cases which, unless special circumstances apply, are not expected to occur. When the above special θ values are excluded, it can be shown [22,23] that by means of a coordinate transformation of the form

$$z_n' = z_n + \gamma_1 z_n^2 + \gamma_2 z_n z_n^* + \gamma_3 (z_n^*)^2, \tag{37}$$

where γ_1, γ_2, and γ_3 are complex numbers, all quadratic terms can be eliminated from Eq. (4b) with $x=0$, yielding

$$z_{n+1}' = \lambda z_n' + d' |z_n'|^2 z_n' + q + r\nu_n + O(q^2, r^2, rz', qz', pz'^2, z'^4), \tag{38}$$

where $\lambda=(1+p)e^{i\theta}$ and

$$d' = \frac{1-2\lambda}{\lambda(\lambda-1)} ab + \frac{\lambda}{\lambda-1} bb^* + \frac{2\lambda}{\lambda^3-1} cc^* + d. \tag{39}$$

Defining $\tilde{z}=z'+q/(1-\lambda)$, and substituting into Eq. (38) cancels q in lowest significant order. Thus, in terms of $\tilde{z}$, Eq. (38) becomes

$$\tilde{z}_{n+1} = \lambda \tilde{z}_n + d' |\tilde{z}_n|^2 \tilde{z}_n + r\nu_n + O(q^2, r^2, r\tilde{z}, q\tilde{z}, p\tilde{z}^2, \tilde{z}^4). \tag{40}$$

Until we consider noise in Sec. V C, we assume that $r=0$. Then Eq. (40) can be transformed into the following canonical form:

$$\begin{pmatrix} |\tilde{z}_{n+1}| \\ \arg(\tilde{z}_{n+1}) \end{pmatrix} = \begin{pmatrix} (1+p)|\tilde{z}_n| - f_1 |\tilde{z}_n|^3 \\ \arg(\tilde{z}_n) + \Theta + f_2 |\tilde{z}_n|^2 \end{pmatrix} + O(q^2, q\tilde{z}, \tilde{z}_n^4) \tag{41}$$

with f_1, Θ, and f_2 being real coefficients. Equation (41) shows that the critical issue is the sign of f_1. A positive sign indicates a soft transition and a negative sign indicates a hard transition. As derived in [22], $f_1 = -\mathrm{Re}(\lambda^* d')$ at the bifurcation value $\lambda = e^{i\theta}$, or

$$f_1 = \mathrm{Re}\left[\frac{(1-2e^{i\theta})e^{-2i\theta}}{1-e^{i\theta}} ab \right] + \frac{1}{2} bb^* + cc^* - \mathrm{Re}(de^{-i\theta}). \tag{42}$$

The sign of the above expression determines whether the transition is hard $(f_1<0)$ or soft $(f_1>0)$.

Next we obtain an expression for the maximum burst amplitude for a soft transition in model (4). We assume that f_1 is of order 1, i.e., we are not close to the borderline between hard and soft transitions. Rewriting the radial part of Eq. (41) as

$$|\tilde{z}_{n+1}| - |\tilde{z}_n| = p|\tilde{z}_n| - f_1 |\tilde{z}_n|^3 + O(q^2, q\tilde{z}, \tilde{z}_n^4), \tag{43}$$

we see that, as in the pitchfork case, the maximum burst amplitude $\tilde{\Delta}$ for $|\tilde{z}|$ is

$$\tilde{\Delta} \simeq \sqrt{p/f_1}. \tag{44}$$

This relation is true if $p\Delta = f_1 \Delta^3 \gg \max(q^2, q\tilde{\Delta}, \tilde{\Delta}_n^4)$. Thus the scaling range for Eq. (44) is $|q| \ll p \ll 1$, and, since $z=z' + O(z')^2 = \tilde{z} + O(\tilde{z}^2, q)$, in this range we have $\Delta \simeq \tilde{\Delta} \simeq \sqrt{p/f_1}$. Since our final result does not depend on the mag-

nitude of q in the scaling range specified, the result applies in the case of noise-induced bubbling as well. Figure 7 shows the scaling of the maximum burst amplitude with p. Experimental data are plotted as dots. The solid curve is calculated from Eq. (44).

In the case of noise, we have a soft transition if $f_1>0$ and a hard transition if $f_1<0$. In the case of a soft transition, by arguments similar to the ones in previous sections, we have $\Delta \simeq \sqrt{p/f_1}$ when $r^{2/3} \ll p \ll 1$.

B. Average interburst time: Mismatch

We now derive an expression for the average interburst time in the presence of mismatch ($q>0$) and no noise ($r=0$). Again we consider an orbit starting at $(x,z)=(0,0+0i)$ and use the new coordinates z' to eliminate the quadratic terms. Note that the coefficient in front of the cubic term in the transformed coordinates is given by Eq. (39). As in the previous derivations (Secs. III and IV), we make use of the fact that, in the case of a hard transition, when $|z_n|$ grows to the point where the nonlinear terms become significant, the nonlinearity pushes $|z_n|$ to $O(1)$ rapidly. Consider the linear terms in map (38), $z_{n+1}=\lambda z_n+q+O(z_n^3)$. We first find the number of iterates it takes to escape starting at 0. Starting at $z=0$, the nth iterate of the linearized map is $z_n=[(1-\lambda^{n+1})/(1-\lambda)]q$. The nonlinear term becomes significant when, after $\bar{n}$ iterates, $|z|$ reaches the critical value $z_c=\sqrt{p/|f_1|}$; thus we have the equation for $\bar{n}$:

$$\left|\frac{1-\lambda^{\bar{n}+1}}{1-\lambda}q\right|^2 \simeq \frac{p}{|f_1|}. \tag{45}$$

Solving the above equation, we find $\bar{n}$:

$$\bar{n} \simeq \frac{1}{2p}\ln\left|\frac{p(1-\lambda)^2}{|f_1||q|^2}\right|. \tag{46}$$

Knowing the number of iterates $\bar{n}$ it takes to escape assuming x_n stays close to the fixed point, we use Eq. (35), $\ln\tau \sim h_\parallel n$, to derive the scaling with p of the average interburst time τ,

$$\ln\tau \sim h_\parallel \bar{n} \simeq \frac{h_\parallel}{2p}\ln\left|\frac{p(1-\lambda)^2}{|f_1||q|^2}\right|. \tag{47}$$

Finally, using the approximation $\lambda=(1+p)e^{i\theta}\simeq e^{i\theta}$, we obtain the final scaling given in Table III:

$$\ln\tau \sim h_\parallel \bar{n} \simeq \frac{h_\parallel}{2p}\ln\left|\frac{p(1-e^{i\theta})^2}{|f_1||q|^2}\right|. \tag{48}$$

We numerically iterated the map (4) starting at a typical irrational x and $z=0+0i$ and measured the interburst time. Figure 8 shows the result of numerical experiments (diamonds); $\ln\tau$ is plotted vs $\bar{n}(p)$, where $\bar{n}(p)$ is given in terms of p by Eq. (48). The solid line has the predicted slope $h_\parallel=\ln 2$ and is consistent with the data.

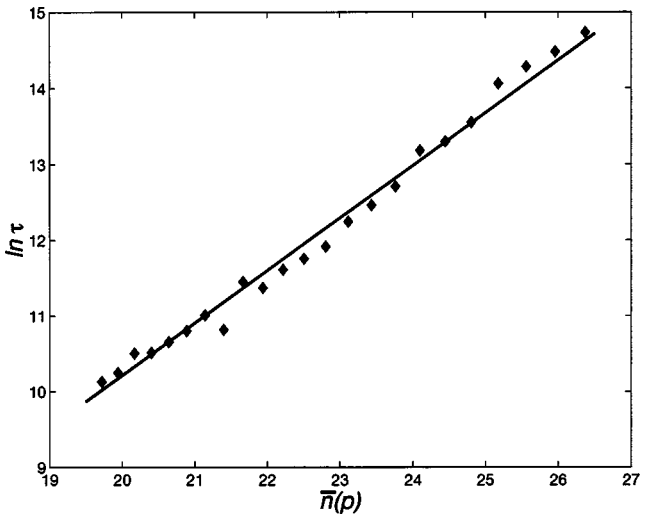

FIG. 8. This plot shows $\ln\tau$ vs $\bar{n}(p)$, where $\bar{n}(p)$ is given by Eq. (46), for bubbling induced by a Hopf bifurcation with asymmetry for $|q| \ll p \ll 1$. Parameter values are $a=1$, $b=1$, $c=1$, $d=2$, $p=0.1,\ldots,0.15$, $\theta=\pi\sqrt{5}$, and $q=0.015$. The experimental data are plotted as diamonds. The solid curve has slope $\ln 2$ predicted by Eq. (48).

C. Average interburst time: Noise

We now consider the case where bubbling is induced by noise, i.e., $r>0$, but $q=0$. According to Eq. (41), for small p and in the presence of noise, the evolution of the radial part of z_n with $x=0$ is the same as the evolution of y in the pitchfork case with cubic nonlinearity with $-f_1$ as the cubic coefficient:

$$|\tilde{z}_{n+1}| \simeq (1+p)|\tilde{z}_n| - f_1|\tilde{z}_n|^3 + r\{\nu_n\}_z. \tag{49}$$

The noise term $r\{\nu_n\}_z$ is the projection of noise in the direction of z_n in the complex plane. Since the noise is distributed uniformly within the unit circle, $\{\nu_n\}_z$ has a one-dimensional probability distribution on $[-1,1]$ with probability distribution function given by $2\sqrt{1-\{\nu\}_z^2}$. This distribution has variance of 1/4. We can analyze Eq. (49) in the same way as in Sec. III C, but with $D=(1/2)r^2\,\mathrm{Var}(\{\nu_n\}_z)$. The θ dependence disappears from the final scaling due to the fact that the distribution of noise is uniform within the unit circle.

Our final results for Hopf bifurcation induced bubbling transitions are summarized in Table III.

VI. FURTHER DISCUSSION OF THE NOISE-INDUCED BUBBLING MECHANISM

In this section we provide more insight into the nature of two types of noise-induced bubbling: noise dominated and drift dominated. Consider again the map (2). We define a critical value y_c such that for $y>y_c$ the nonlinear terms become dominant and the burst quickly follows. A burst occurs when x comes close to the fixed point $x=0$ and stays there for a large number of iterates $\bar{n}$. The probability per iterate of that event is of order $\exp(-h_\parallel\bar{n})$. After x has entered the required vicinity of the fixed point, the linear coefficient

$\cos(2\pi x)+p \simeq 1+p$ immediately starts driving y away from the invariant manifold. At the time x enters the region near $x=0$, y will typically be of the order of the size of the noise, $y \sim r$. Thus a burst will occur if $y_c \sim r \exp(\overline{n}p)$, or $\overline{n} \sim p^{-1} \ln(y_c/r) \sim p^{-1}$. We call this scenario drift-dominated bubbling. The probability per iterate of initiating a burst by this mechanism is of order $\exp(-h_\parallel/p)$ and goes to zero exponentially as p comes close to the critical value $p=0$. This would imply that bursts do not happen when $p=0$, but the experimental results suggest otherwise. Thus we consider another possible route for a burst that becomes important when p sufficiently small. We call this second mechanism noise-dominated bubbling. In the noise-dominated case p is close enough to zero that it can be ignored. In that case a burst may occur if x comes close to the fixed point $x=0$ and stays there for $\overline{n}$ iterates where $\overline{n}$ is in the range $y_c/r \lesssim \overline{n} \lesssim (y_c/r)^2$. With p neglected, the probability of reaching y_c in $\overline{n}$ iterates is of order $\exp[-(y_c^2/\overline{n}r^2)]$. This the probability of a burst in this case is of order $\exp[-(y_c^2/\overline{n}r^2)]\exp(-\overline{n}h_\parallel)$, which is maximized when $\overline{n} \sim y_c/r$. This suggests that when such a burst occurs the noise behaves *coherently* over $\overline{n}$ iterates pushing y on average in the same direction away from the invariant manifold. Since we determined y_c for a coherent perturbation to be proportional to $r^{1/\sigma}$ [see Eq. (12) and discussion in Sec. III B], the probability of the burst becomes of order $\exp(-h_\parallel r^{(1-\sigma)/\sigma})$. Thus the average interburst time τ is of order

$$\tau \sim \min(\exp(h_\parallel r^{(1-\sigma)/\sigma}), \exp(h_\parallel/p)). \tag{50}$$

Equation (50) suggests that the noise-induced bursting mechanism prevails if $p^{\sigma/(\sigma-1)}/|r| \ll 1$, while the drift-induced bursting mechanism prevails if $p^{\sigma/(\sigma-1)}/|r| \gg 1$.

VII. CONCLUSION

The above discussions have assumed that there is no attractor away from the invariant manifold. In the situation where there is an attractor away from the invariant manifold, our analytical results derived in Secs. III–V still apply, but the meaning of τ is different. Specifically, for the case that we previously referred to as a hard transition, q, $r=0$ now yields a riddled basin attractor on the invariant manifold [4,10]. For q, $r \neq 0$ this attractor is destroyed and converted to a chaotic transient whose mean lifetime is given by τ (Tables I–III).

To summarize, in this work we have presented a unified treatment of the bubbling transitions involving all generic types of bifurcation: pitchfork, transcritical, period doubling, and Hopf. We have theoretically derived results for scalings of the average interburst time and the maximum burst amplitude with the normal parameter as well as conditions for hard and soft bubbling transitions in the above three cases for both noise- and mismatch-induced bubbling.

ACKNOWLEDGMENTS

This research was supported by the Office of Naval Research (Physics), the National Science Foundation (Divisions of Mathematical and Physical Sciences), and the W. M. Keck Foundation. Our interest in this problem was originally motivated by interesting discussions with D. Gauthier concerning his experiments on coupled chaotic oscillators.

APPENDIX

In this Appendix we provide details of the solution of Eq. (20) subject to the boundary conditions $\overline{P}(\pm y_c, s)=0$. We look for an approximate solution in terms of a perturbation expansion $\overline{P}(y,s)=\overline{P}_0(y,s)+p\overline{P}_1(y,s)+O(p^2)$. First, we set $p=0$ in Eq. (20) to obtain an equation for $\overline{P}_0(y,s)$:

$$D\frac{\partial^2 \overline{P}_0}{\partial y^2} - s\overline{P}_0 = -\delta(y). \tag{A1}$$

The solution of this equation satisfying the boundary conditions is

$$\overline{P}_0(y,s) = \frac{\sinh[(y_c-|y|)\sqrt{s}/\sqrt{D}]}{2\sqrt{Ds}\cosh(y_c\sqrt{s}/\sqrt{D})}. \tag{A2}$$

Now since we know $\overline{P}_0(y,s)$, we can deduce the equation for $\overline{P}_1(y,s)$:

$$D\frac{\partial^2 \overline{P}_1}{\partial y^2} - y\frac{\partial \overline{P}_0}{\partial y} - \overline{P}_0 - s\overline{P}_1 = 0. \tag{A3}$$

Solving the above equation subject to boundary conditions $\overline{P}_1(\pm y_c, s)=0$ and $(\partial \overline{P}_1/\partial y)_{y=0}=0$, we obtain the expression for $\overline{P}_1(y,s)$:

$$\overline{P}_1(y,s) = \frac{[1-(s/D)|y|^2+\sqrt{s/D}y_c\tanh(\sqrt{s/D}y_c)]\sinh[\sqrt{s/D}(|y|-y_c)]+\sqrt{s/D}(y_c-|y|)\cosh[\sqrt{s/D}(|y|-y_c)]}{8\cosh(\sqrt{s/D}y_c)}. \tag{A4}$$

Upon setting $s=h_\parallel$ and substitution of the expressions for $\overline{P}_0(y,s)$ and $\overline{P}_1(y,s)$ into Eq. (21) and integration over y we obtain

$$\ln \tau \sim -\ln\left[\frac{1+py_c^2/(4D)-[py_c/(4\sqrt{h_\parallel D})]\tanh(\sqrt{h_\parallel}y_c/\sqrt{D})}{\cosh(\sqrt{h_\parallel}y_c/\sqrt{D})}\right]. \tag{A5}$$

The quantity $\sqrt{h_\parallel}y_c/\sqrt{D}$ in Eq. (A5) is large, which allows us to make the approximations $\cosh(\sqrt{h_\parallel}y_c/\sqrt{D}) \simeq \exp[\sqrt{h_\parallel}y_c/\sqrt{D}]/2$ and $\tanh(\sqrt{h_\parallel}y_c/\sqrt{D}) \simeq 1$, and neglect the $y_c/(4\sqrt{h_\parallel D})$ term compared to $y_c^2/(4D)$, to obtain the final scaling given in Eq. (22).

[1] A manifold is invariant if every initial condition in the manifold remains in the manifold.

[2] In on-off intermittancy, the invariant surface is on average unstable and exhibits bursting, which occurs in the absence of noise or mismatch. A. S. Pikovsky, Z. Phys. B: Condens. Matter **55**, 149 (1984); H. Fujisaka and H. Yamada, Prog. Theor. Phys. **75**, 1088 (1986); L. Yu, E. Ott and Q. Chen, Phys. Rev. Lett. **65**, 2935 (1990); N. Platt, E. A. Spiegel, and C. Tresser, *ibid.* **70**, 279 (1993); S. C. Venkataramani, T. M. Antonsen, E. Ott, and J. C. Sommerer, Phys. Lett. A **207**, 173 (1995).

[3] J. C. Alexander, I. Kan, J. Yorke, and Z. You, Int. J. Bifurcation Chaos **2**, 795 (1992).

[4] P. Ashwin, J. Biescu, and I. Stewart, Phys. Lett. A **193**, 126 (1994).

[5] J. F. Heagy, T. L. Carroll, and L. M. Pecora, Phys. Rev. E **52**, R1253 (1995).

[6] D. J. Gauthier and J. C. Bienfang, Phys. Rev. Lett. **77**, 1751 (1996).

[7] S. C. Venkataramani, B. R. Hunt, and E. Ott, Phys. Rev. E **54**, 4819 (1996).

[8] S. C. Venkataramani, B. R. Hunt, E. Ott, D. J. Gauthier, and J. C. Bienfang, Phys. Rev. Lett. **77**, 5361 (1996).

[9] E. Ott and J. C. Sommerer, Phys. Lett. A **188**, 39 (1994).

[10] E. Ott, J. C. Sommerer, J. C. Alexander, I. Kan, and J. A. Yorke, Phys. Rev. Lett. **71**, 4134 (1993); J. C. Sommerer and E. Ott, Nature (London) **365**, 136 (1993); Y. C. Lai *et al.*, Phys. Rev. Lett. **77**, 55 (1996).

[11] D. Sweet, Phys. Plasmas (to be published).

[12] L. M. Pecora and T. L. Carroll, Phys. Rev. Lett. **64**, 821 (1990).

[13] B. R. Hunt and E. Ott, Phys. Rev. Lett. **76**, 2254 (1996).

[14] In case (i), the pitchfork bifurcation is generic for systems that are symmetric about the invariant manifold, while the transcritical bifurcation is generic for systems without symmetry. A saddle-node bifurcation is not possible, because it would destroy the periodic orbit, whereas the normal parameter does not affect the dynamics in the invariant manifold.

[15] S. Yanchuk, Y. Maistrenko, and E. Mosekilde, Physica D **154**, 26 (2001).

[16] S.-Y. Kim and W. Lim, Phys. Rev. E **63**, 026217 (2001); S.-Y. Kim, W. Lim and Y. Kim, Prog. Theor. Phys. **105**, 187 (2001); S.-Y. Kim and W. Lim, Phys. Rev. E **64**, 016211 (2001).

[17] S.-Y. Kim, W. Lim, A. Jalnine, and S. P. Kuznetsov (unpublished).

[18] A. Jalnine and S.-Y. Kim, Phys. Rev. E **65**, 026210 (2002).

[19] S.-Y. Kim, W. Lim, and Y. Kim, Prog. Theor. Phys. **107**, 2 (2002).

[20] J. Hale and H. Kocak, *Dynamics and Bifurcations* (Springer-Verlag, New York, 1991).

[21] *Handbook of Mathematical Functions*, edited by M. Abramowitz and I. A. Stegun (Dover, New York, 1965).

[22] Y.-H. Wan, SIAM (Soc. Ind. Appl. Math.) J. Appl. Math. **34**, 1 (1978).

[23] O. Lanford, *Nonlinear Problems in the Physical Sciences and Biology* (Springer-Verlag, New York, 1973).